

LIMIT STATES FOR PIPES UNDER COMBINED LOADS

Paulo Pedro Kenedi¹, pkenedi@cefet-rj.br
Lavinia Maria Sanábio Alves Borges², lavinia@mecanica.coppe.ufrj.br
Murilo Augusto Vaz³, murilo@peno.coppe.ufrj.br

¹PPEMM - Programa de Pós-Graduação em Engenharia Mecânica e Tecnologia dos Materiais - CEFET/RJ - Av. Maracanã, 229 - Maracanã - RJ - CEP 20271-110 - Brasil

²PEM - Programa de Engenharia Mecânica - COPPE/UFRJ - Av. Brigadeiro Trompowsky, s/n, Ilha do Fundão - RJ - CEP 21940-900 - Brasil

³PEnO - Programa de Engenharia Oceânica - COPPE/UFRJ - Av. Brigadeiro Trompowsky, s/n, Ilha do Fundão - RJ - CEP 21940-900 - Brasil

Abstract. *Pressurized pipes submitted to combined loads can fail by bursting, excessive ovalization, ratcheting, local and/or global buckling, unstable fracture, plastic collapse and impact. In this work onshore pipes are submitted to axial, in-plane bending and internal pressure loads. The effect of several loads combinations are analyzed through the utilization of a series of yield locus patterns. They are used to avoid combinations of loads that could cause plastic collapse or global buckling.*

Keywords: *yield locus, limit states, plastic collapse, global buckling*

1. INTRODUCTION

Limit analysis theory can be used to predict plastic collapse of structures submitted to any loading combination. On the contrary of incremental plasticity approach, the limit analysis theory allows the determination of incipient collapse load without considering strain history or any kind of material behavior evolution. An incipient plastic collapse could occur if an equilibrated and plastically admissible stress field coexists with a field of unbounded pure plastic strain. The load that equilibrates a collapse stress field is denoted Collapse Load or Plastic Limit Load.

The application of limit analysis theory in several structures has been studied, as in Kim (2007). He did finite element limit analysis for pipes submitted to bend and internal pressure. Paquette (2006) analyzed pipe buckling under internal pressure and axial compression, conducting tests at an experimental setup as well as by developing an analytic approach. Bardi and Kyriakides (2006) analyzed pipe plastic buckling under axial compression with experimental and analytic results. Robertson *et al.* (2005) stated that there are three main types of failure that must be considered for the design of pipes: gross plastic deformation, ratcheting and fatigue. Chattopadhyay (2002) studied the effect of internal pressure for in-plane collapse bending moment of pipes. Mohareb (2001) through the utilization of yield locus curves studied the interaction of several loads as axial and shear forces, bending and twisting moments and internal pressure, at fully plastic failure of pipes. Kim and Oh (2006b) and Hauch and Bai (1998) made finite element analysis, obtained experimental results and proposed analytic solutions to analyze local buckling and plastic collapse of pipes. Wierzbicki and Sinmao (1997) analyzed the Brazier effect for plastic bending of pipes using analytic and finite element approaches.

In this work is done an organized review of main models of yield locus of pipes available in technical literature. It is organized by type of loading: axial, internal and external pressures and bending moment. The combination of several loadings is also presented. For compression load a simple global buckling model is presented. The differences of performance caused by pipe's ends, open or closed, are accessed as well as, the influence of internal pressure to a pipe loaded by axial force and bending moment. A model is proposed and its results are compared with Hauch and Bai (1999) model, used as reference.

2. REVIEW

A review of representative yield locus models is done for pipes submitted to different loadings. The yield locus models are used, in constitutive part of limit analysis theory, to calculate the plastic collapse failure. Kyriakides and Corona (2007), Bai (2001), Borges (1991), Lubliner (1990) and Hodge (1959) can be used to assess a more complete approach about theory and applications of limit analysis. In this work the original expressions collected from referenced literature are adapted to generate dimensionless expressions. The dimensionless bending moment M , axial load N and internal pressure P_i are represented, respectively, by m , n and p . Also the load that yields entirely the pipe cross section submitted to M , N and P_i are represented, respectively, by M_0 , N_0 and P_0 .

The dimensionless expressions used in this work are:

$$m = \frac{M}{M_0} \quad n = \frac{N}{N_0} \quad p = \frac{P_i}{P_0} \quad (01)$$

$$M_0 = 4r_m^2 t \sigma_y \quad N_0 = 2\pi r_m t \sigma_y \quad P_0 = \frac{t}{r_m} \sigma_y \text{ (open-ended)} \quad (02)$$

Where, r_m is the average radius, t is the wall thickness and σ_y is the yield strength.

In sequence several representative yield locus models are shown. Each loading mode are shown as axial, internal pressure, external pressure and bending moment. The combination of two or more loading modes are also presented.

For **pure axial load**:

Hauch and Bai (1999) states:

$$N = SMTS A \quad \text{or} \quad n = 1 \quad (03)$$

For this particular case $N_0 = SMTS A$, where A is the cross sectional area. Note that $2\pi r_m t$ of expression (02.b) is a good approximation of A for pipes with small t/r_m ratio. $SMTS$ is the specified minimum tensile strength, which is the longitudinal stress at failure.

For **pure internal pressure**:

A pipe can fails by internal pressure. (API, 1999 *apud* Hauch and Bai, 1999, p.4) states that:

$$P_i = \frac{t}{r_m} [0.5(SMTS + SMYS)] \quad \text{or} \quad p = 1 \quad (04)$$

For this particular case, $P_0 = \frac{t}{r_m} [0.5(SMTS + SMYS)]$, where $0.5(SMTS + SMYS)$ is the hoop stress at failure. $SMYS$ is the specified minimum yield strength.

For **pure external pressure**:

(Timoshenko, 1961 *apud* Hauch and Bai, 1999, p.3) uses a lower bound model to estimate the pressure that yields a pipe external fibers:

$$P_c^2 - \left[P_p + \left(1 + 1.5 \frac{f_0 D_m}{t} \right) P_{el} \right] P_c + P_p P_{el} = 0 \quad (05)$$

$$P_{el} = \frac{2E}{(1-\nu^2)} \left(\frac{t}{D_m} \right)^2, \quad P_p = 2 SMYS \left(\frac{t}{D_m} \right) \quad \text{and} \quad f_0 = \frac{D_{max} - D_{min}}{D_m} \quad (06)$$

Where, P_c is the characteristic collapse pressure, P_p is the plastic buckling pressure, P_{el} is the elastic buckling pressure, f_0 is the initial out of roundness, E is the Young Modulus, ν is the Poisson ratio, D_{min} and D_{max} are, respectively, the minimum and the maximum diameters.

(Haagsma, 1981 *apud* Hauch and Bai, 1999, p.4) estimate, by using an upper bound model, the pressure that causes fully plastic yielding for external collapse pressure:

$$P_c^3 - P_{el} P_c^2 - \left[P_p^2 + P_{el} P_p f_0 \frac{D}{t} \right] P_c + P_{el} P_p^2 = 0 \quad (07)$$

The utilization of (06) and (07) expressions is granted for pipes whose material is initially linear elastic and for elastic buckling pressures derived from classical analysis.

For pure bending moment:

(SUPERB, 1996 *apud* Hauch and Bai, 1999, p.3) shows that as bending moment increase the cross section ovalization increase as well. The result is a decrease of moment of inertia which could be compensated, in some extent, by the pipe material strain hardening:

$$M = \left(1.05 - 0.0015 \frac{2r_m}{t}\right) 4 SMYS r_m^2 t \quad \text{or} \quad m = \left(1.05 - 0.0015 \frac{2r_m}{t}\right) \quad (08)$$

For this particular case, $M_0 = 4 SMYS r_m^2 t$. Also the term $\left(1.05 - 0.0015 \frac{2r_m}{t}\right)$ represent the average longitudinal cross sectional stress in function of radius and wall thickness of pipe.

For small displacement analysis and ideal plastic material, (Calladine, 1974 *apud* Chattopadhyay, 2002, p.134) state, for a lower bound model, the bending moment of a thin curved pipe, using elastic shell analysis and limit theorems of plasticity:

$$M = 0.935 \lambda^{2/3} (4r_m^2 t \sigma_y) \quad \text{for} \quad \lambda < 0.5 \quad \text{or} \quad m = 0.935 \lambda^{2/3} \quad \text{for} \quad \lambda < 0.5 \quad (09)$$

$$\lambda = \frac{R t}{r_m^2} \quad (10)$$

Where R is the bend radius and λ is the pipe bend characteristic (a non-dimensional variable). For small displacement analysis and ideal plastic material, (Spence and Findlay, 1973 *apud* Chattopadhyay, 2002, p.134) utilized previous analyses and limit theorems of perfect plasticity to estimate approximate bounds of limit bending moments:

$$M = \begin{cases} 0.8 \lambda^{0.6} (4r_m^2 t \sigma_y) & \text{for} \quad \lambda < 1.45 \\ 4r_m^2 t \sigma_y & \text{for} \quad \lambda \geq 1.45 \end{cases} \quad \text{or} \quad m = \begin{cases} 0.8 \lambda^{0.6} & \text{for} \quad \lambda < 1.45 \\ 1 & \text{for} \quad \lambda \geq 1.45 \end{cases} \quad (11)$$

For large displacement analysis (Goodall, 1978 *apud* Chattopadhyay, 2002, p.134) estimate, for closing mode, the limit bending moments for thin elbows:

$$M = \frac{1.04 \lambda^{2/3}}{1 + \beta} (4r_m^2 t \sigma_y) \quad \text{or} \quad m = \frac{1.04 \lambda^{2/3}}{1 + \beta} \quad (12)$$

$$\beta = \left(2 + \frac{(3\lambda)^{2/3}}{3}\right) \left(\frac{4\sqrt{3(1-\nu^2)} \sigma_y r_m}{\pi E t}\right) \quad (13)$$

Where, β is a correction factor. (Touboul el al., 1989 *apud* Chattopadhyay, 2002, p.135) shows, based in an experimental study at CEA DEMENT:

$$M = 0.715 \lambda^{2/3} (4r_m^2 t \sigma_y) \quad \text{or} \quad m = 0.715 \lambda^{2/3} \quad \text{for closing mode} \quad (14.a)$$

$$M = 0.722 \lambda^{1/3} (4r_m^2 t \sigma_y) \quad \text{or} \quad m = 0.722 \lambda^{1/3} \quad \text{for opening mode} \quad (14.b)$$

Where closing and opening modes are related with the direction of bending of curved pipes, as in Kim and Oh (2006a). (Drubay el al., 1995 *apud* Chattopadhyay, 2002, p.135) stated:

$$M = 0.769 \lambda^{2/3} (4r_m^2 t \sigma_y) \quad \text{or} \quad m = 0.769 \lambda^{2/3} \quad \text{for closing mode} \quad (15)$$

Also, (Chattopadhyay, 2002 *apud* Kim and Oh, 2006a, p.1445, 1447) shows:

$$m = 1.075 \lambda^{2/3} \quad \text{for closing mode} \quad (16.a)$$

$$m = 1.048 \lambda^{1/3} - 0.0617 \quad \text{for opening mode} \quad (16.b)$$

The range of m for the models of pure bending locus, for typical values of λ of 0.2 and 0.5, can be estimated to the following ranges: $\lambda = 0.2 \rightarrow 0.24 < m < 0.55$ and $\lambda = 0.5 \rightarrow 0.45 < m < 0.77$.

For combined load:

Authors as Bardi and Kyriakides (2006), Chattopadhyay (2000) and Bai and Moan (1997) have already published combined load results. Also Hauch and Bai (1999) show the interaction between M , N and P in the capacity of pipes to resist plastic collapse, generating the following yield locus expression:

$$\frac{M}{M_0} = \sqrt{1 - (1 - \alpha^2) \left(\frac{P}{P_0}\right)^2} \cos \left(\frac{\pi}{2} \frac{\frac{N}{N_0} - \alpha \frac{P}{P_0}}{\sqrt{1 - (1 - \alpha^2) \left(\frac{P}{P_0}\right)^2}} \right) \quad \text{or} \quad m = \sqrt{1 - (1 - \alpha^2) p^2} \cos \left(\frac{\pi}{2} \frac{n - \alpha p}{\sqrt{1 - (1 - \alpha^2) p^2}} \right) \quad (17)$$

$$\alpha = 0.25 \frac{P_c}{N_0} \quad (\text{for external overpressure}) \quad \text{or} \quad \alpha = 0.25 \frac{P_0}{N_0} \quad (\text{for internal overpressure}) \quad (18)$$

Where, α is a correction factor obtained through the utilization of finite element analysis, as in Hauch and Bai (1999). Another yield locus for combined loading for allowable bending moment and local buckling under load controlled mode was proposed by Hauch and Bai (1999):

$$\frac{M}{M_0} = \frac{\eta_{RM}}{\gamma_C} \sqrt{1 - (1 - \alpha^2) \left(\frac{P}{\eta_{RP} P_0}\right)^2} \cos \left(\frac{\pi}{2} \frac{\frac{\gamma_C}{\eta_{RF}} \frac{N}{N_0} - \alpha \frac{P}{\eta_{RP} P_0}}{\sqrt{1 - (1 - \alpha^2) \left(\frac{P}{\eta_{RP} P_0}\right)^2}} \right) \quad (19)$$

Where, η_{RM} , η_{RP} and η_{RF} are strength usage factors and are based in standards as DNV and the engineering experience of Seren Hauch and Yong Bai. γ_C is the condition load factor.

Finally there are shown two models which combine M and P but not N . Using small displacement analysis (Goodall., 1978 *apud* Kim and Oh, 2006a, p.1444), proposed a yield locus expression for open-ended elbows under combined loading of internal pressure and in-plane bending:

$$M = 4 t r_m^2 \sigma_y \left(1.04 \lambda^{2/3} \left(1 - P \frac{r_m}{t \sigma_y} \right) \right)^{1/3} \quad \text{or} \quad m = (1 - p)^{1/3} \quad (20)$$

For this particular case, $M_0 = 4 t r_m^2 \sigma_y \left(1.04 \lambda^{2/3} \right)$.

Another yield locus model for combined loads was proposed by Chattopadhyay (2002) for opening and closing in-plane bending for $0.24 \leq \lambda \leq 0.6$ and $0.0 \leq p \leq 1.0$:

$$m = 1.122 \lambda^{2/3} + 0.175 \frac{p}{\lambda} - 0.508 p^2 \quad \text{for closing mode} \quad (21.a)$$

$$m = 1.047 \lambda^{1/3} + 0.124 \frac{p}{\lambda^{1.2}} - 0.568 p^2 \quad \text{for opening mode} \quad (21.b)$$

The Hauch and Bai (1999) combined load model for plastic collapse, expression (17.b), will be used, in this work, as reference model.

3. PROPOSED MODEL

At Kenedi *et al.* (2009) and Kenedi (2008) present the main aspects of limit analysis theory, which include equations of equilibrium, kinematics and constitutive relations for straight and curved pipes submitted to concentrated or distributed loads. The proposition of a yielding function that includes internal pressure (as a dead load) is done as well. The material is considered elastic-perfectly plastic and it is supposed that the loading generates small deformation.

A pipe segment submitted to a combination of tensile axial load N , positive bending moment M and internal pressure P is shown at Figure 1, as well the cross section area and the geometrical variables of a thin-walled pipe.

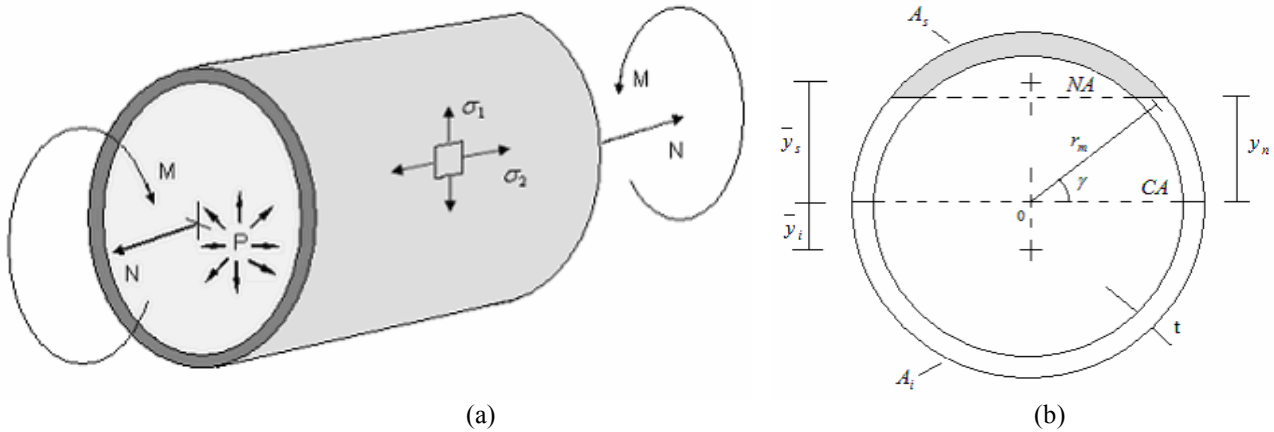


Figure 1. (a) Pipe segment submitted to load combination and (b) cross section area of a thin-walled pipe for tensile axial load and positive bending moment.

Where, CA and NA are respectively centroidal and neutral axis, y_n is the distance from CA to NA . The transversal area A is divided in two areas by NA , the superior area A_s (shaded at Fig.1.b) and the inferior area A_i . \bar{y}_s is the distance between centroid of area A (shown with a 0) and the centroid of A_s and \bar{y}_i is the distance between centroid of area A and the centroid of A_i . γ is an angle ranging from $-\frac{\pi}{2}$ to $\frac{\pi}{2}$ rad. The minor area is approximated by $(\pi - 2\gamma)t r_m$ and the major area is approximated by $(\pi + 2\gamma)t r_m$. At fig. 1.b the minor area is A_s and corresponds to the shaded area. The minor distance is $\left(\frac{2 \cos(\gamma)}{\pi + 2\gamma}\right) r_m$ and the major distance is $\left(\frac{2 \cos(\gamma)}{\pi - 2\gamma}\right) r_m$.

The pipe segment equilibrium, submitted to tensile axial force, positive bending moment and internal pressure, shown at Figure 1.a, with the utilization of von Mises criterion, is used to obtain the yielding function expressions.

$$\left(\frac{\sigma_1}{\sigma_y}\right)^2 - \frac{\sigma_1 \sigma_2}{\sigma_y \sigma_y} + \left(\frac{\sigma_2}{\sigma_y}\right)^2 = 1 \quad \text{and} \quad \sigma_1 = p P_0 \frac{r_m}{t} \quad (22)$$

$$P_0 = \frac{t}{r_m} \sigma_y \quad (\text{open-ended}) \quad \text{or} \quad P_0 = \frac{2}{\sqrt{3}} \frac{t}{r_m} \sigma_y \quad (\text{closed-ended}) \quad (23)$$

For open-ended pipes, applying (22.a), (22.b), (01.c) and (23.a), σ_2/σ_y can be cast as:

$$\frac{\sigma_2}{\sigma_y} = \frac{p}{2} \pm \sqrt{1 - \frac{3}{4} p^2} \quad \text{or} \quad \frac{\sigma_t}{\sigma_y} = \frac{p}{2} + \sqrt{1 - \frac{3}{4} p^2}, \quad \frac{\sigma_c}{\sigma_y} = \frac{p}{2} - \sqrt{1 - \frac{3}{4} p^2} \quad \text{for} \quad p \leq |1| \quad (24)$$

For closed-ended pipes, applying (22.a), (22.b), (01.c) and (23.b), σ_2/σ_y can be cast as:

$$\frac{\sigma_2}{\sigma_y} = \frac{p}{\sqrt{3}} \pm \sqrt{1 - p^2} \quad \text{or} \quad \frac{\sigma_t}{\sigma_y} = \frac{p}{\sqrt{3}} + \sqrt{1 - p^2}, \quad \frac{\sigma_c}{\sigma_y} = \frac{p}{\sqrt{3}} - \sqrt{1 - p^2} \quad \text{for} \quad p \leq |1| \quad (25)$$

Where σ_1 and σ_2 are principal stresses, σ_t and σ_c are, respectively, the stresses at tensile and compressive areas.

Figure 2 shows a graphical representation of expressions (24.b), (24.c), (25.b) and (25.c):

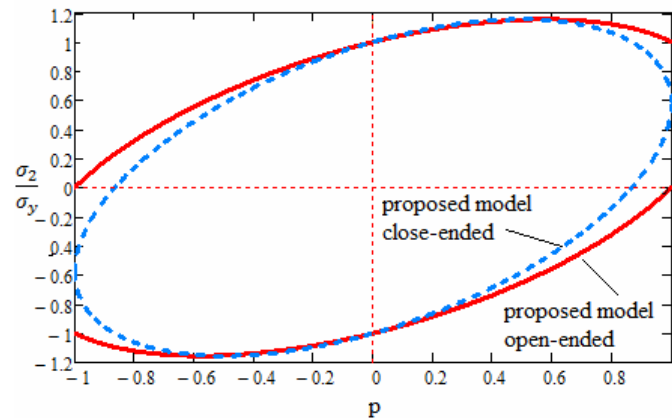


Figure 2. Locus of normalized principal stresses, σ_2/σ_y , function of p .

Figure 2 shows the maximum values of σ_2/σ_y for various levels of normalized internal pressure, for two ends patterns: closed and open. For $p = 0$ both curves has the same performance and they are limited at $p = |1|$.

For $p \neq 0$ the behavior of the two patterns differentiates, with open-ended pipe (continuous red curves) reaching higher levels of σ_2/σ_y and p , than pipes with closed-ended (dashed blue curve). The equilibrium expressions for open-ended pipe can be cast, using (24.b) and (24.c). For $\sigma_s = \sigma_c$ and $\sigma_i = \sigma_t$:

$$\begin{cases} \sigma_s A_s + \sigma_i A_i = N \\ -\sigma_s A_s \bar{y}_s + \sigma_i A_i \bar{y}_i = M \end{cases} \quad (26)$$

The equilibrium expressions for closed-ended pipe can be cast, using (25.b) and (25.c), as:

$$\begin{cases} \sigma_s A_s + \sigma_i A_i = N + \pi r_m^2 P \\ -\sigma_s A_s \bar{y}_s + \sigma_i A_i \bar{y}_i = M \end{cases} \quad (27)$$

Solving (26), the yield locus of open-ended pressurized pipe submitted to axial and in-plane bending loads is obtained:

$$m = \pm \sqrt{1 - \frac{3}{4} p^2} \cos \left[\frac{\pi}{2} \frac{\left(n - \frac{p}{2} \right)}{\sqrt{1 - \frac{3}{4} p^2}} \right] \quad (\text{open-ended}) \quad (28)$$

Similarly, solving (27) for closed-ended pipe:

$$m = \pm \sqrt{1 - p^2} \cos \left[\frac{\pi}{2} \frac{n}{\sqrt{1 - p^2}} \right] \quad (\text{closed-ended}) \quad (29)$$

For a particular case of null axial load ($n = 0$) expressions (28) and (29), can be rewritten respectively, as:

$$m = \pm \sqrt{1 - \frac{3}{4} p^2} \cos \left[\frac{\pi}{2} \frac{\frac{p}{2}}{\sqrt{1 - \frac{3}{4} p^2}} \right] \quad (\text{open-ended}) \quad (30)$$

$$m = \pm \sqrt{1 - p^2} \quad (\text{closed-ended}) \quad (31)$$

Figure 3 shows a graphical representation of expressions (30) and (31):

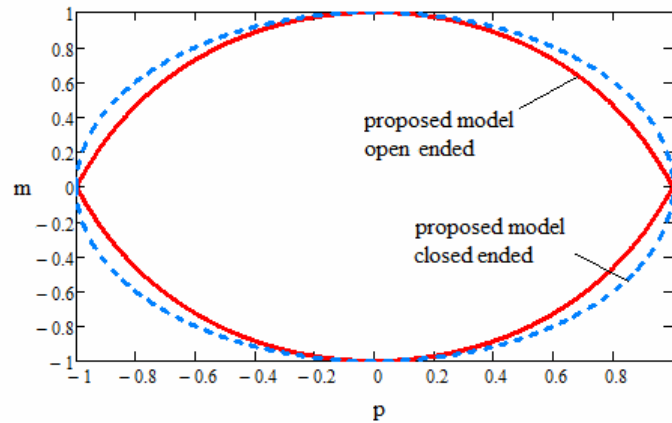


Figure 3. Proposed model with different endings yield locus graphic m versus p , for $n = 0$.

Figure 3 shows the yield locus of the proposed model, for $n = 0$, with different endings. For $p = -1$, $p = 0$ and for $p = 1$ both curves have the same performance. For $-1 < p < 1$ the closed-ended (dashed blue curve) permits higher combinations of m and p than open-ended (continuous red curve). For a particular case of null internal pressure, $p = 0$, the expressions (28) and (29) can be cast as:

$$m = \pm \cos\left[\frac{\pi}{2} n\right] \tag{32}$$

To analyze the influence of termination of pipes Figure 4 was generated. It shows the yield locus curves, respectively for open and closed-ended pipes, calculated from the application of expressions (28) and (29), submitted to a combination of bending moment M , axial load N and internal pressure P :

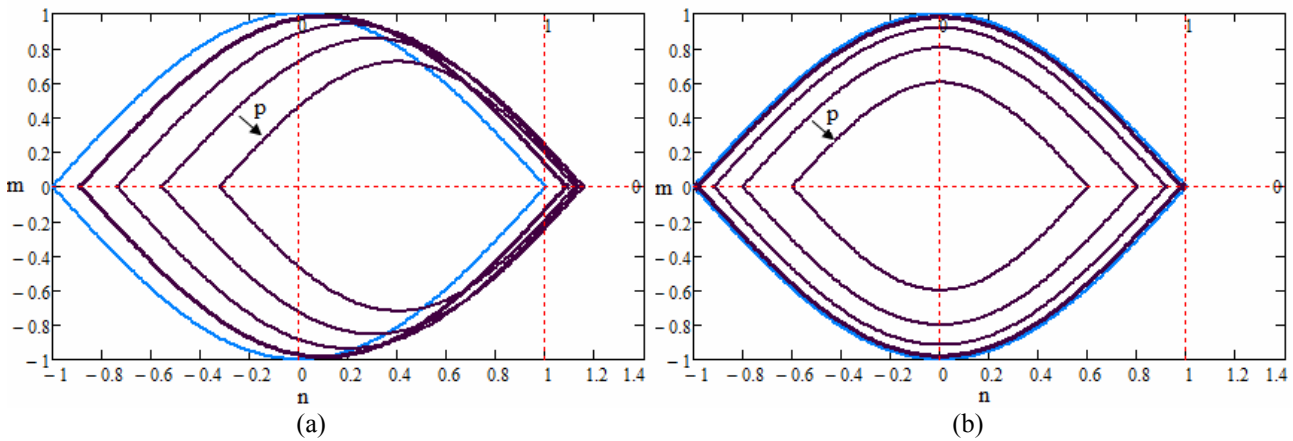


Figure 4. Limiting yielding surfaces for pipes with: (a) open-ended and (b) closed-ended.

Figure 4 presents two graphics for values of m versus n , for normalized pressures $0 \leq p \leq 0.8$, with increments of $0.2p$. Note that the arrows shows direction that p increases. At Figures 4.a and 4.b, for $p = 0$ the limiting yielding surfaces are the large ones (blue curves). As p increases the limiting yielding surfaces become smaller. For open-ended pipes the limiting yielding surfaces moves to the right side of the graph, while for closed-ended pipes the limiting yielding surfaces maintain concentric.

Although the determination of a combined load yield locus is fundamental to estimation of plastic collapse of a pipe, the global buckling failure is also very important. There are two types of global buckling: the load-controlled, that can induce a catastrophic failure and the displacement-controlled, that usually is not so dangerous. Plastic collapse and global buckling are concurrent failure modes, so it is possible, if there are compressive axial load, that a pipe can fails by global buckling before failing by plastic collapse.

The Euler's formula, as in Crandall *et al.* (1978), can be applied to estimate the dimensionless axial load pipe global buckling n_B , in load-controlled condition. It is supposed that both ends are pivoted.

$$\frac{d^2y}{dx^2} + \frac{N}{EI}y = -\frac{M}{EI} \quad (33)$$

Where I is the moment of inertia. At $L/2$, where L is the length of pipe, the transversal displacement is maximum, y_{\max} :

$$y_{\max} = \frac{M}{N} \left(\sec \left(\sqrt{\frac{N}{EI}} \frac{L}{2} \right) - 1 \right) \quad (34)$$

When the secant argument is $\pi/2$, the displacement is infinite, generating the critical axial load N_{crit} :

$$N_{crit} = \frac{\pi^2 EI}{L^2} \quad (35)$$

Note that if the pipe ends is not modeled as pivoted, then (35) has to be multiplied by end-condition constant as in Crandall *et al.* (1978). Also note that although (34), the displacement expression, depends on M and N , the critical axial load not depends of M . Using (02.a), (02.b) and (35), the normalized axial load, n_B , which the pipe buckles can be estimated:

$$n_B = \frac{N_{crit}}{N_0} = \frac{\pi EI}{2r_m t L^2 \sigma_y} \quad (36)$$

Figure 5 shows a classical example of yield locus of plastic collapse for $p = 0$. At same figure the global buckling locus is represented by blue vertical lines (dashed or continuous). The geometric characteristics used to generate this figure were obtained from Hauch and Bai (1999). Several multiples of lengths L were used, with $L = 12$ m.

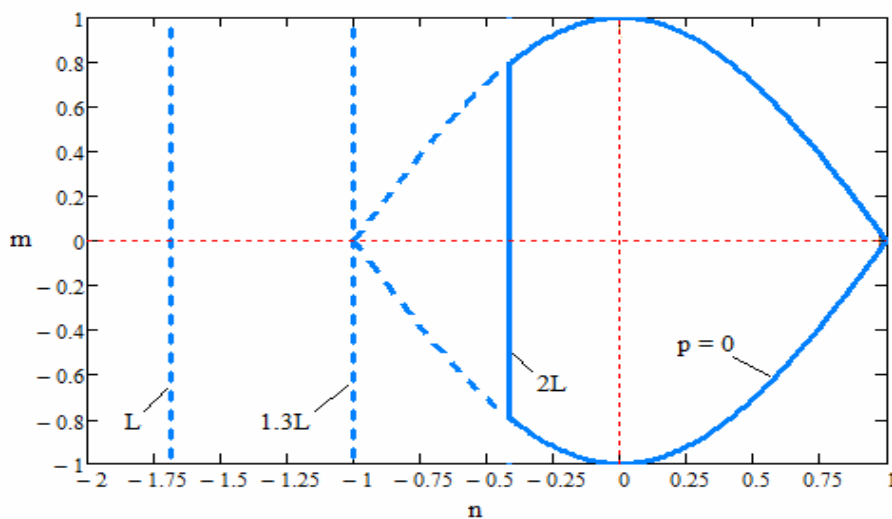


Figure 5. Plastic collapse (for $p = 0$) and global buckling yield locus for open-ended pipe.

Figure 5 shows several critical normalized axial loads n_B , represented by vertical lines, for multiple pipes lengths. Note that dashed blue lines have insufficient length to buckle the pipe. For this example $1.3L$ is the maximum pipe length that the failure occur first by plastic collapse. The vertical blue line, marked as $2L$, limits the yield locus to the region at the right side of it. As expected, as the pipe's length L becomes larger larger the vertical blue line dislocate to the right, with an obvious limit for $n = 0$.

At Figure 6 are shown two yield locus, for $p = 0$ and $p = 0.8$, for open-ended pipe.

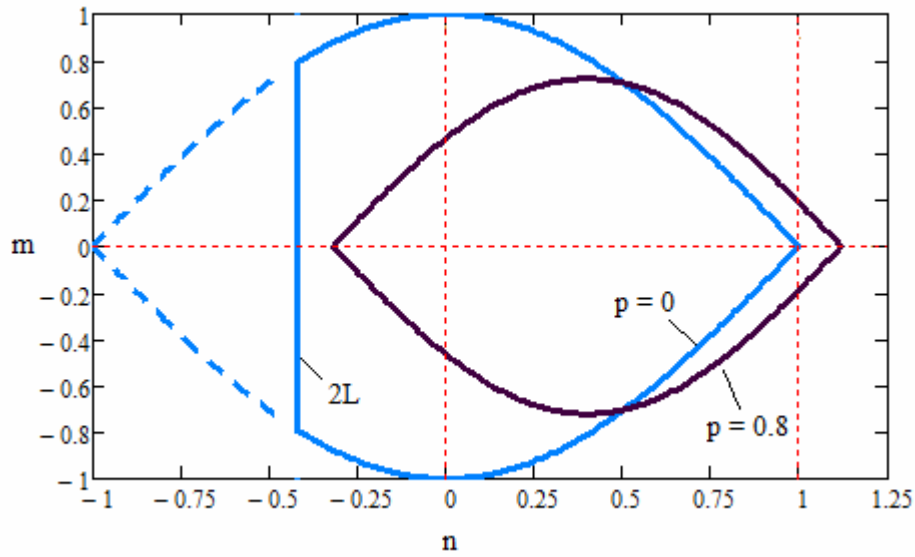


Figure 6. Plastic collapse, for $p = 0$ and $p = 0.8$, and global buckling yield locus for $2L$ open-ended pipe length.

Comparing the yield locus curves for $p = 0$ and $p = 0.8$, for a pipe with $2L$ length, is interesting to note that for $p = 0$ there is a region that buckle before fails by plastic collapse, while for $p = 0.8$, the pipe only fails by plastic collapse.

4. COMPARISON

The proposed model for open-ended (28) was compared with the Hauch and Bai model (17.b), used in this work as reference. The results is shown graphically at Figure 7.

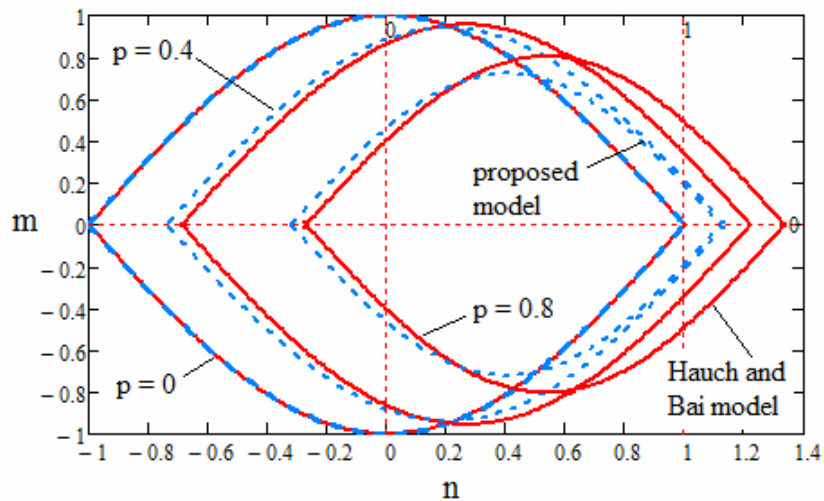


Figure 7. Comparative yield locus of Hauch and Bai and proposed models.

For $p = 0$, the bigger yield locus, the two models have a perfect match, where the Hauch and Bai model is represented by a continuous red line and the proposed model is represented by a dashed blue line. Also for compressive n they are close. For tensile n , for $p \neq 0$, there are significant differences between models, that increase as p increases.

Nevertheless, both models the yield locus curves moves to the right side of the graph and become smaller as p increases. Note that, at this figure, the global buckling limitations not are shown.

5. CONCLUSIONS

A review of yield locus models for different load combinations was assessed. A model to determine the yield locus of pressurized pipes, for open and closed-ended, submitted to combined loadings of axial force, bending moment and internal pressure was presented. Especial cases of no internal pressure or no axial force were analyzed. The effect of global buckling was also added. Finally the proposed model with open-ended pipe was compared with a reference model with reasonable agreement, mainly for n compressive. The results shows that the yield locus of combined loading for open-ended pipes for both models, proposed and reference, dislocates to the right side of yield locus figure as internal pressure became higher. This phenomena affects directly the capacity of pipe, submitted to $n < 0$, to resist to global buckling, increasing its capacity as the internal pressure increases.

6. REFERENCES

- Bai, Y., Iglan, R.T. and Moan, T., 1997, "Tube Collapse Under Combined External Pressure, Tension and Bending", *Marine Structures*, Vol. 10, pp. 389-410.
- Bai, Y., 2001, "Pipelines and Risers", Volume 3, Elsevier Ocean Engineering Book Series.
- Bardi, F.C. and Kyriakides, S., 2006, "Plastic buckling of circular tubes under axial compression - part I: Experiments", *International Journal of Mechanical Sciences*, Vol. 48, pp. 830-841.
- Bardi, F.C., Kyriakides, S. and Yun, H.D., 2006, "Plastic buckling of circular tubes under axial compression - part II: Analysis", *International Journal of Mechanical Sciences*, Vol. 48, pp. 842-854.
- Borges, L.M.S.A., 1991, "Formulação e solução para análise limite com superfícies de escoamento não linear", Tese de Doutorado, PUC - Rio, Rio de Janeiro, Brasil.
- Chattopadhyay, J., 2000, "Closed-form collapse moment equations of elbows under combined internal pressure and in-plane bending moment", *Journal of Pressure Vessel Technology*, Vol. 122, pp. 431-436.
- Chattopadhyay, J., 2002, "The effect of internal pressure on in-plane collapse moment of elbows", *Nuclear Engineering and Design*, Vol. 212, pp. 133-144.
- Crandall, S.H., Dahl, N. C. and Lardner, T.J., 1978, "An Introduction to the Mechanics of Solids", Mc Graw-Hill International Editions, 2nd edition with SI Units.
- Hauch, S. and Bai, Y., 1998, "Use of finite element analysis for local buckling design of pipelines", *Proceedings of 17th International Conference on Offshore Mechanics and Arctic Engineering - OMAE98-3907*.
- Hauch, S. and Bai, Y., 1999, "Bending moment capacity of pipes", *Proceedings of 18th International Conference on Offshore Mechanics and Arctic Engineering - OMAE99/PIPE-5037*.
- Hodge, P.G., 1959, "Plastic analysis of structures", Mc Graw Hill.
- Lubliner, J., 1990, "Plasticity theory", McMillan Publishing Company.
- Kenedi, P.P., 2008, "Análise limite em dutos", Tese de Doutorado, COPPE-UFRJ, Rio de Janeiro, Brasil.
- Kenedi, P.P., Borges, L.M.S.A. and Vaz, M.A., 2009, "Plastic Collapse of Pressurized Pipes", *Proceedings of 30th Cilamce, Armação dos Búzios, Brasil*.
- Kim, Y. and Oh, C., 2006a, "Closed-form plastic collapse loads of pipe bends under combined pressure and in-plane bending", *Engineering Fracture Mechanics*, Vol. 73, pp. 1437-1454.
- Kim, Y. and Oh, C., 2006b, "Limit loads for pipe bends under combined pressure and in-plane bending based on finite element limit analysis", *International Journal of Pressure Vessels and Piping*, Vol. 83, pp. 148-153.
- Kim, Y. and Oh, C., 2007, " Effects of attached straight pipes on finite element limit analysis for pipe bends", *International Journal of Pressure Vessels and Piping*, Vol. 84, pp. 177-184.
- Kyriakides, S. and Corona, E., 2007, "Mechanics of Offshore Pipelines", volume1: buckling and collapse, Elsevier.
- Mohareb, M., 2001, "Exact yield hyper-surface for thin pipes", *International Journal of Pressure Vessels and Piping*, Vol. 78, pp. 507-514.
- Paquette, J.A. and Kyriakides, S., 2006, "Plastic buckling of tubes under axial compression and internal pressure", *International Journal of Mechanical Sciences*, Vol. 48, pp. 855-867.
- Robertson, A., Li, H. and Mackenzie, D., 2005, "Plastic collapse of pipe bends under combined internal pressure and in-plane bending", *International Journal of Pressure Vessels and Piping*, Vol. 82, pp. 407-416.
- Wierzbicki, T. and Sinmao, M.V., 1997, "A simplified model of brazier effect in plastic bending of cylindrical tubes", *International Journal of Pressure Vessels and Piping*, Vol. 71, pp.19-28.

7. RESPONSIBILITY NOTICE

The authors are the only responsible for the printed material included in this paper.